

1 **Lateral gene transfer drives metabolic flexibility in the anaerobic**
2 **methane oxidising archaeal family *Methanoperedenaceae***

3 Andy O. Leu^a, Simon J. McIlroy^a, Jun Ye^a, Donovan H. Parks^a, Victoria J. Orphan^b, Gene W.
4 Tyson^{a,#}

5 ^aAustralian Centre for Ecogenomics, School of Chemistry and Molecular Biosciences,
6 University of Queensland, Brisbane, Australia

7 ^bDepartment of Geological and Planetary Sciences, California Institute of Technology,
8 Pasadena, CA 91106, USA

9

10 Running Head: Metabolic diversity of the *Methanoperedenaceae*

11 # Address correspondence to: Gene W. Tyson, g.tyson@uq.edu.au.

12 Andy O. Leu and Simon J. McIlroy contributed equally to this work. Author order reflects the
13 order in which the authors joined the project.

14 Abstract word count: 246

15 Article word count: 5216

16

17 **Abstract**

18 Anaerobic oxidation of methane (AOM) is an important biological process responsible for
19 controlling the flux of methane into the atmosphere. Members of the archaeal family
20 *Methanoperedenaceae* (formerly ANME-2d) have been demonstrated to couple AOM to the
21 reduction of nitrate, iron, and manganese. Here, comparative genomic analysis of 16
22 *Methanoperedenaceae* metagenome-assembled genomes (MAGs), recovered from diverse
23 environments, revealed novel respiratory strategies acquired through lateral gene transfer
24 (LGT) events from diverse archaea and bacteria. Comprehensive phylogenetic analyses
25 suggests that LGT has allowed members of the *Methanoperedenaceae* to acquire genes for
26 the oxidation of hydrogen and formate, and the reduction of arsenate, selenate and elemental
27 sulfur. Numerous membrane-bound multi-heme *c* type cytochrome complexes also appear to
28 have been laterally acquired, which may be involved in the direct transfer of electrons to
29 metal oxides, humics and syntrophic partners.

30

31 **Importance**

32 AOM by microorganisms limits the atmospheric release of the potent greenhouse gas
33 methane and has consequent importance to the global carbon cycle and climate change
34 modelling. While the oxidation of methane coupled to sulphate by consortia of anaerobic
35 methanotrophic (ANME) archaea and bacteria is well documented, several other potential
36 electron acceptors have also been reported to support AOM. In this study we identify a
37 number of novel respiratory strategies that appear to have been laterally acquired by members
38 of the *Methanoperedenaceae* as they are absent in related archaea and other ANME lineages.
39 Expanding the known metabolic potential for members of the *Methanoperedenaceae*

40 provides important insight into their ecology and suggests their role in linking methane
41 oxidation to several global biogeochemical cycles.

42

43 **Introduction**

44 Anaerobic oxidation of methane (AOM) is an important microbiological process moderating
45 the release of methane from anoxic waters and sediments into the atmosphere (1-4). Several
46 diverse uncultured microbial lineages have been demonstrated to facilitate AOM. The
47 bacterium “*Candidatus Methyloirabilis oxyfera*” is proposed to couple AOM to
48 denitrification from nitrite, generating oxygen from nitric oxide for the activation of methane
49 (5). Different lineages of anaerobic methanotrophic (ANME) archaea are hypothesised to
50 mediate AOM through the reversal of the methanogenesis pathway and conserve energy
51 using mechanisms similar to those found in methylotrophic and acetoclastic methanogens (6).
52 Unlike methanogens, most of these ANMEs encode a large repertoire of multi-heme *c*-type
53 cytochromes (MHCs), which are proposed to mediate direct interspecies electron transfer to
54 syntrophic sulfate-reducing bacteria (SRB)(7, 8), and/or the reduction of metal oxides and
55 humic acids (9-12).

56 Currently, several clades within the archaeal phylum Euryarchaeota have been shown to be
57 capable of anaerobic methanotrophy and include ANME-1a-b, ANME-2a-c,
58 *Methanoperedenaceae* (formerly known as ANME-2d), and ANME-3 (refs. 13, 14, 15).

59 Marine ANME lineages are often observed to form consortia with SRBs, with ANME-1 and
60 ANME-2 (a,b, and c) being associated with multiple genera within Desulfobacterales and
61 *Desulfobulbaceae* (13, 16-20), thermophilic ANME-1 with “*Candidatus Desulfofervidus*
62 *auxilii*” (8, 21) and ANME-3 with SRBs of the *Desulfobulbus* (22). While members of the
63 family *Methanoperedenaceae* have also recently been associated with SRB of the family

64 *Desulfobulbaceae* in a freshwater lake sediment (23), they also appear to oxidise methane
65 independently using a range of electron acceptors. The type species of this family,
66 “*Candidatus Methanoperedens nitroreducens*”, was originally enriched in a bioreactor and
67 shown to couple AOM to the reduction of nitrate via a laterally transferred nitrate reductase
68 (15). Subsequently, “*Ca. Methanoperedens* sp. BLZ1” was also found to encode a laterally
69 transferred nitrite reductase, which is also present in the genome of “*Ca. M nitroreducens*”,
70 potentially allowing these microorganisms to couple AOM to dissimilatory nitrate reduction
71 to ammonia (DNRA) (24). More recently, three novel species belonging to the
72 *Methanoperedenaceae* were enriched in bioreactors demonstrated to couple AOM to the
73 reduction of insoluble iron or manganese oxides (9, 12). These microorganisms did not
74 encode dissimilatory nitrate reduction pathways, but instead were inferred to use multiple
75 unique MHCs during metal-dependent AOM to facilitate the transfer of electrons to the metal
76 oxides (9, 12), consistent with the extracellular electron transfer mechanisms proposed for
77 marine ANME (7, 8). Bioreactor performance and 16S rRNA gene amplicon data has also
78 been used to suggest that members of the *Methanoperedenaceae* are capable of AOM
79 coupled to the reduction of selenate and chromium(VI), although this remains to be
80 confirmed with more direct evidence (25, 26). Notably, members of the
81 *Methanoperedenaceae* have been observed to facilitate AOM coupled to multiple terminal
82 electron acceptors within the same natural sediment (27). Individual members of the family
83 can possess such metabolic flexibility, with a lab-enriched species shown to couple AOM to
84 the reduction of nitrate, iron and manganese oxides (10). Given the relatively poor genomic
85 representation of the *Methanoperedenaceae*, and the lack of detailed physiological studies of
86 its members, it is likely that considerable metabolic diversity for the lineage remains to be
87 discovered.

88 In this study, comparative analysis was conducted on 16 *Methanoperedenaceae* metagenome-
89 assembled genomes (MAGs) recovered from various environments to investigate the
90 metabolic diversity and versatility of the family and to understand the evolutionary
91 mechanisms responsible for these adaptations. These analyses indicate that members of the
92 *Methanoperedenaceae* have acquired a large number of genes through LGT that potentially
93 allow AOM to be coupled to a wide range of electron acceptors, suggesting their role in
94 methane oxidation extends beyond environments with nitrate and metal oxides.

95

96 **Results and Discussion**

97 *Expanding the genomic representation of the Methanoperedenaceae*

98 In order to explore the metabolic diversity within the *Methanoperedenaceae*, comparative
99 genomic analysis was performed on both publicly available and newly acquired MAGs
100 (**Table 1**). The publicly available genomes include five MAGs recovered from bioreactors
101 where AOM is coupled to the reduction of nitrate (“*Ca. Methanoperedens nitroreducens*”;
102 *M.Nitro* (15), and “*Ca. Methanoperedens sp. BLZ2*”; BLZ2 (ref. 28)), iron (“*Ca.*
103 *Methanoperedens ferrireducens*”; *M.Ferri* (9)) and manganese (“*Ca. Methanoperedens*
104 *manganicus*” and “*Ca. Methanoperedens manganireducens*”, Mn-1 and Mn-2, respectively
105 (12)). Also included are two environmental MAGs recovered from groundwater samples
106 from the Horonobe and Mizunami underground research laboratories in Japan (HGW-1 and
107 MGW-1) (29, 30), and one MAG from an Italian paddy soil sample (IPS-1) (31). In order to
108 recover additional genomes belonging to the family, GraftM (32) was used to screen public
109 metagenome sequence datasets from NCBI for *Methanoperedenaceae*-related 16S rRNA and
110 *mcrA* gene sequences. Subsequent assembly and genome binning on datasets found to contain
111 *Methanoperedenaceae*-like sequences led to the recovery of an additional eight MAGs

112 belonging to the family. Six of these were from arsenic contaminated groundwater samples
113 (ASW-1-6), and a further two from sediment and groundwater samples from a copper mine
114 tailings dam (CMD-1 and CMD-2). All 16 MAGs are highly complete ($\geq 87.4\%$) with low
115 contamination ($\leq 5.9\%$) based on 228 Euryarchaeota-specific marker genes (**Table 1**)(33).
116 These genomes vary in GC content from 40.2 to 50.7% and range in size from 1.45 to 3.74
117 Mbp.

118 A genome tree including 1,199 publicly available archaeal genomes, based on a concatenated
119 set of 122 marker genes (34), confirmed the phylogenetic placement of the 16 MAGs within
120 the *Methanoperedenaceae*. The genome tree supports that these MAGs form a monophyletic
121 clade sister to the GoM-Arc1 genomes (**Figure 1**). These genomes likely represent three
122 separate genera within the family, based on their placement within a reference tree, relative
123 evolutionary distance, FastANI distance, and average amino acid identity (AAI (35); 61.3 to
124 89.2%; **Figure S1**). All MAGs were classified as members of the genus “*Ca.*
125 *Methanoperedens*”, except HGW-1 and ASW-3 which appear to represent independent genus
126 level lineages (**Figure 1**). Phylogenetic analysis of the six MAGs containing 16S rRNA genes
127 was consistent with the genome tree (**Figure S2**), supporting their classification as members
128 of the *Methanoperedenaceae* family.

129

130 *Potential electron donors used by the Methanoperedenaceae*

131 Metabolic reconstruction of the *Methanoperedenaceae* MAGs showed that all genomes
132 encoded the central methanogenesis pathway, inclusive of the methyl-coenzyme M reductase,
133 supporting their potential for the complete oxidation of methane to CO₂ (**Figures 2 and S3**).
134 The annotation of membrane-bound formate dehydrogenases (FdhAB) in five of the
135 *Methanoperedenaceae* MAGs (Mn-2, ASW-4, ASW-1, MGW-1, and BGW-1; **Figure 3**)

136 suggests that some members of the family may also oxidise formate (E_0 [CO₂/HCOO⁻] = -
137 430 mV) (36). As the enzyme is reversible, these species could also potentially produce
138 formate as a supplementary electron sink during AOM. Formate was suggested as a putative
139 electron shuttle between ANME-1 and their syntrophic partner SRB, based on the annotation
140 and expression of an *fdhAB* in ANME-1, but this has not been supported with physiological
141 studies (37, 38). The putative formate dehydrogenase encoded in the Mn-2 MAG is
142 phylogenetically related to an FdhA found in the genome of *Caldiarchoaeum subterraneum*,
143 while those encoded by ASW-4, ASW-1, MGW-1, and BGW-1 appear to be more similar to
144 the FdhA of *Methanocellaceae* archaeon UBA148 (**Figure 3**).

145 The use of hydrogen (H₂; E_0 = -414mV (39)) as an electron source was previously suggested
146 for MGW-1 and HGW-1 which encode Group 1 membrane-bound NiFe hydrogenase
147 complexes, composed of a NiFe catalytic subunit, a FeS electron transfer subunit, and a
148 membrane-bound *b*-type cytochrome (29, 30). These hydrogenases, along with similar Group
149 1 NiFe hydrogenases identified in the ASW-6 and CMD-2 MAGs, form a monophyletic clade
150 with those encoded by the MAG for “*Ca. Hydrothermarchaeota*” (JdFR-18), which belongs
151 to the archaeal phylum Hydrothermarchaeota (40), and several members of the Halobacterota
152 (**Figure S4A**). The ASW-3 and ASW-5 MAGs encode Group 1 NiFe hydrogenases that are
153 basal to Vho/Vht/Vhx hydrogenases encoded by members of the genus *Methanosarcina* (41).
154 As the ASW-5 NiFe hydrogenase does not encode a *b*-type cytochrome (**Figure S4B**), it is
155 unclear how electrons are derived from hydrogen. In addition to the membrane-bound NiFe
156 hydrogenases, the M.Nitro MAG was found to encode genes for two different sets of Group
157 3b cytoplasmic hydrogenases (**Figure S4A**). The MGW-1 (ref. 29) and ASW-2 MAGs also
158 encode Group 3b hydrogenases which have been implicated in hydrogen evolution and
159 nicotinamide adenine dinucleotide phosphate (NADPH) reduction (42). Similar complexes
160 have also been shown to have hydrogen oxidation and elemental sulfur reducing capabilities

161 (42-44). It is unknown how these Group 3b hydrogenases would contribute to energy
162 conservation given their predicted cytoplasmic localisation. The functionality of the
163 annotated Group 1 and 3 NiFe hydrogenases is supported by the identification of the NiFe
164 binding motifs (L1 and L2) on their NiFe catalytic subunits and the annotation of all or most
165 of the hydrogenase maturation genes (hypA-F) on the same *Methanoperedenaceae* MAGs
166 (**Dataset S1D**). The potential for some *Methanoperedenaceae* to couple the oxidation of
167 hydrogen and/or formate to the reduction of exogenous electron acceptors would be
168 advantageous with the dynamic availability of methane in natural environments (45).

169

170 *Pathways for energy conservation during AOM in the Methanoperedenaceae*

171 All members of the *Methanoperedenaceae* encode the Fpo complex
172 (FpoABCDHIJ₁J₂LMNOF), a homolog of Complex I (nuoABCDEFGHijklmn), which is
173 hypothesised to oxidize F₄₂₀H₂ coupled to the reduction of a membrane-bound soluble
174 electron carrier, and translocation of two protons out of the cell (**Figures 2 and S5A**) (41, 46).
175 While members of the *Methanosarcinales* and marine ANME-2a are reported to typically use
176 methanophenazine (MP) as their membrane-bound soluble electron carrier, the
177 *Methanoperedenaceae* and ANME-1 have previously been suggested to use menaquinone
178 (MK) based on the annotation of the futasine pathway for MK biosynthesis in several
179 MAGs representing these lineages (47). Comparative genomic analysis of the 16
180 *Methanoperedenaceae* MAGs revealed that the futasine pathway is a conserved feature of
181 all members, except the most basal member ASW-3 (see later; **Dataset S1A**). As has
182 previously been suggested by Arshad *et al.*, (48), the larger difference in redox potential
183 between F₄₂₀ ($E_0 = -360\text{mV}$) and MK ($E_0 = -80\text{mV}$ (49)), relative to F₄₂₀ and MP ($E_0 = -$
184 165mV (50)), would theoretically allow the Fpo complex to translocate more protons

185 (3H⁺/2e⁻) out of the cell for every molecule of F₄₂₀ oxidised, giving a higher overall energetic
186 yield from AOM (**Figure S5B**).

187 Phylogenetic analysis of the Fpo complex in the *Methanoperedenaceae* MAGs showed that
188 the FpoKLMNO subunits are homologous to proteins found in MP utilising members of the
189 *Methanosarcinales*. The FpoABCDHIJ₁J₂ subunits are more similar to those found in
190 microorganisms known to use MK and other quinones, which have more positive redox
191 potentials (**Figures S5 and S6; Dataset S1E**) (51). As the latter subunits (specifically FpoH)
192 are responsible for interaction with the membrane soluble electron carrier pool (52, 53), this
193 observation provides further support to the use of MK by members of the
194 *Methanoperedenaceae*. To our knowledge, this is the first reported example of a lineage
195 encoding a ‘hybrid’ Complex I homolog possessing subunits with homology to those found
196 in phylogenetically diverse microorganisms (**Figure S6**). The GoM-Arc-I MAGs appear to
197 possess the MK biosynthesis pathway and a similar ‘hybrid’ Fpo complex to the
198 *Methanoperedenaceae* (**Figure S6**), suggesting that the evolutionary adaptation of the lineage
199 to utilise MK occurred prior to the divergence of these two related families. Members of the
200 GoM-Arc-1 clade possess Mcr-like complexes (**Figure S3**) and are suggested to use short-
201 chain alkanes – possibly ethane (54, 55). Interestingly, the FpoMNO subunits of the ASW-3
202 MAG cluster with those of the other members of the *Methanoperedenaceae* family, while
203 their FpoABCDHIJ₁J₂KL subunits are most similar to those of the ANME-2a and other
204 members of the *Methanosarcinales* (**Figure S6**). While the genes involved in MP
205 biosynthesis are not known, the absence of the MK biosynthesis pathway indicate that ASW-
206 3 likely uses MP. As the most basal lineage of this family, ASW-3 may have adapted to use
207 MP after the evolutionary divergence of the GoM-Arc-I and *Methanoperedenaceae*, although
208 further genomic representation of this lineage is required to verify this hypothesis.

209 Comparative genomic analyses of the *Methanoperedenaceae* MAGs revealed that none of
210 these genomes encode an Rnf complex, which is hypothesised to re-oxidise ferredoxin
211 coupled to the transport of sodium ions out of the cell and the reduction of MP in marine
212 ANME-2a (7, 56) and other methylotrophic methanogens (41, 57, 58). In the absence of this
213 complex, ferredoxins could be re-oxidised with a ‘truncated’ Fpo complex, similar to the Fpo
214 complex possessed by *Methanosaeta thermophila* (59). Alternatively an electron confurcating
215 mechanism could be used for the re-oxidation of ferredoxin, coenzyme M, and coenzyme B,
216 coupled to the reduction of two F₄₂₀ via a cytoplasmic complex composed of a heterodisulfide
217 reductase (HdrABC) and a F₄₂₀ hydrogenase subunit B (FrhB) (24). The two additional
218 F₄₂₀H₂ could subsequently be fed back into the Fpo complex, greatly increasing the overall
219 bioenergetic yield (24) (**Figure 2**). All of the *Methanoperedenaceae* MAGs have the genetic
220 potential for these alternate strategies for re-oxidation of ferredoxin during AOM, however,
221 further experimental validation is required to test these hypotheses.

222

223 *Conservation of unique menaquinone: cytochrome c oxidoreductases within the*

224 *Methanoperedenaceae*

225 Five different putative MK:cytochrome c oxidoreductase gene clusters (**Figures 1 and 2;**
226 **Dataset S1A**) that are hypothesised to mediate the transfer of electrons out of the cytoplasmic
227 membrane were identified in the *Methanoperedenaceae* MAGs. These gene clusters include a
228 non-canonical bc1/b6f complex adjacent to two hypothetical proteins and two 6-haem multi-
229 heme cytochromes (MHCs; Group 1), two clusters where a *b*-type cytochrome is adjacent to
230 a 6-haem MHC (Groups 2 and 3), and another two clusters where a NrfD-like transmembrane
231 protein is adjacent to an electron transferring 4Fe-4S ferredoxin iron-sulfur protein and
232 MHCs (Groups 4 and 5; **Figure 2**). These bc and NrfD complexes are frequently found in

233 other metal reducing microorganisms and mediate electron transport from the cytoplasm to
234 the periplasm (60-62).

235 Most of the 16 *Methanoperedenaceae* MAGs (except CMD-1 and ASW-3) have more than
236 one of these MK:cytochrome oxidoreductase complexes and 11 have at least four (**Figure 1**).
237 ASW-3 is the only MAG not to encode any MK: cytochrome *c* oxidoreductases, which is
238 consistent with its putative use of MP. A gene encoding a cytochrome-*b* found to be most
239 similar to “*Ca. Methanohalarchaeum thermophilum*” was identified in ASW-3; however, in
240 the absence of a collocated MHC gene, the extracellular electron transfer step for this
241 microorganism is unclear.

242 Phylogenetic analysis of the membrane-bound subunits of the MK:cytochrome *c*
243 oxidoreductases (**Figure 2**), which include the NrfD subunits (from Groups 1 and 2) and the
244 *b*-type cytochromes (from Groups 3, 4 and 5), showed that they have been potentially
245 laterally transferred from diverse donors (**Figure S7**). The *Methanoperedenaceae* NrfD
246 subunits formed independent clusters with sequences from members of the
247 Dehalococcoidales family RBG-16-60-22 (Group 1) and a single MAG (RBG-16-55-9) from
248 the candidate phylum Bipolaricaulota (Group 2; **Figure S7A**). The *b*-type cytochromes of the
249 *Methanoperedenaceae* belong to three distinct clades (**Figure S7B**). The *b*-type cytochromes
250 from Groups 3 and 4 clustered with proteins from GoM-ArcI, indicating vertical genetic
251 inheritance from an ancestor of these two families, and Group 5 proteins clustered with those
252 from the class Archaeoglobi (40).

253 The conservation of multiple conserved laterally transferred MK:cytochrome *c*
254 oxidoreductases in most of the *Methanoperedenaceae* MAGs may contribute to the reported
255 ability for members of the family to reduce a variety of electron acceptors with a range of
256 redox potentials that include Fe(III) oxide reduction (-100mV to 100mV) (63), nitrate

257 (+433mV)(24), and Mn(IV) (+380mV) (36). Transcriptomic analyses has shown that
258 different MK:cytochrome *c* oxidoreductases are expressed in different species of the genus
259 “*Ca. Methanoperedens*” during AOM coupled to the reduction of Fe(III) oxides (9), Mn(IV)
260 oxides (12), and nitrate (15, 24). A similar phenomenon is observed for the species
261 *Geobacter sulfurreducens*, where different extracellular electron pathways were used when
262 reducing different electron acceptors (64).

263

264 *Potential electron acceptors used by the Methanoperedenaceae*

265 Annotation of the *Methanoperedenaceae* MAGs revealed a wide array of genes associated
266 with previously undescribed respiratory strategies for the family that appear to have been
267 acquired via LGT. Principally, these are putative terminal oxidoreductase complexes
268 belonging to the Complex-Iron-Sulfur-Molybdenum (CISM) superfamily that were absent in
269 the genomes of related archaeal lineages (**Figure 3**). These complexes are composed of a
270 catalytic subunit, an iron-sulfur protein, and a membrane-bound subunit, and facilitate the
271 transfer of electrons between the electron acceptor/donor and the MK pool (**Figure 2**).

272 As previously reported, the MAGs M.Nitro, BLZ2, and IPS-1 encode respiratory nitrate
273 reductases that are part of the CISM superfamily, allowing them to independently mediate
274 AOM coupled to nitrate reduction (15, 24, 65). Based on phylogenetic analysis (**Figure 3**),
275 genes encoding cytoplasmic nitrite oxidoreductases (NxrA) were identified in the IPS-1,
276 BLZ2, and M.Nitro MAGs, and a nitrate reductase closely related to NarG proteins was
277 identified in the BLZ2 MAG. Of the *Methanoperedenaceae* MAGs, only the M.Nitro and
278 BLZ2 MAGs possess a putative nitrite reductase (NrfA) for DNRA. The M.Ferri MAG
279 encodes an assimilatory nitrate reductase (NarB/NasA) most similar to a protein encoded by
280 the *Magnetobacterium casensis* (**Figure 3**). However, in the absence of an annotated nitrite

281 reductase in the M.Ferri MAG, the potential of this microorganism for assimilatory nitrate
282 reduction is unclear.

283 Multiple MAGs (ASW-2,3,5,6, and Mn-2) were also found to encode putative selenate
284 reductases (SrdA; **Figure 3**), suggesting their ability for Se(VI)-dependent AOM. Recently, a
285 bioreactor enrichment of a member of the genus “*Ca. Methanoperedens*” exhibited AOM
286 activity when nitrate was substituted with selenate (26). However, as no meta-omic analyses
287 was conducted for the community, it is unclear if the dominant “*Ca. Methanoperedens*”
288 possessed a putative selenate reductase, or if it was directly responsible for the observed
289 selenate reduction.

290 The ASW-1 and ASW-3 MAGs encode a putative sulfur reductase (SreABC). This
291 annotation is supported by its phylogenetic clustering of the catalytic sub-unit with SreA
292 from *Aquifex aeolicus* (**Figure 3**), which has been shown to reduce elemental sulfur, as well
293 as tetrathionate and polysulfide (66). This is the first genomic evidence suggesting that
294 members of the *Methanoperedenaceae* may be involved in respiratory sulfur-dependent
295 AOM and warrants further investigation. ANME-1 have been proposed to couple AOM to the
296 reduction of polysulfide in a biogenic hydrocarbon seep sediment, but this was based on the
297 annotation and high expression of a putative sulfide: quinone oxidoreductase (SQR)(67).

298 Genes for dissimilatory sulfate reduction pathways were absent in the *Methanoperedenaceae*
299 MAGs, consistent with other ANME lineages (68). MGW-1 was recently speculated to
300 directly couple AOM to sulfate reduction utilising assimilatory sulfate reduction pathways.
301 This hypothesis was based on the lack of large MHCs or identifiable alternate electron
302 acceptor complexes encoded in the MAG (29). Several of the *Methanoperedenaceae* MAGs,
303 and those of other ANME lineages, contain candidate genes associated with assimilatory
304 sulfate reduction, but a dissimilatory role for these has not been shown (68).

305 The M.Nitro MAG encodes two putative reductases belonging to the arsenate reductase
306 (ArrA) and arsenite oxidase (ArxA) group (**Figure 3**). The BLZ2, ASW-1, ASW-4, IPS-1
307 MAGs also encode reductases that cluster with the M.Nitro ArxA-like sequence. The ArxA
308 protein has been found to be capable of both arsenite oxidation and arsenate reduction (69),
309 which would allow the *Methanoperedenaceae* possessing these ArxA-like proteins to utilise
310 arsenate as a terminal electron acceptor. Proteins encoded by the ASW-3 and “*Candidatus*
311 *Acetothermum autotrophicum*” (70) (**Figure 3**) form a deep branching clade adjacent to the
312 ArxA and ArrA groups, suggesting these species might also have the potential to respire on
313 arsenic compounds. It is noteworthy that the ASW-1, 3, and 4 MAGs were recovered from a
314 Bangladesh arsenic contaminated groundwater sample (**Table 1**), indicating a role for LGT in
315 their niche-specific adaptation. The possibility of AOM coupled to arsenate (As(V))
316 reduction has important environmental implications given the wide distribution of arsenic in
317 nature, including subsurface drinking water aquifers (71), and the toxicity and mobility of its
318 reduced form, arsenite (As(III)) (72) (73). Arsenic reduction and mobilisation has been linked
319 to an inflow of organic carbon in contaminated aquifers where methane (~1mM) and arsenate
320 co-occur (74, 75).

321 Additional putative oxidoreductases clades that are not closely associated with any well
322 characterised CISM proteins were also found in the *Methanoperedenaceae* MAGs. This
323 includes two proteins encoded by the ASW-3 and ASW-6 MAGs that cluster with a protein
324 of unknown function from a *Brocadiales* MAG (76), and the CMD-1 protein that clusters
325 with a protein from *Brocadia fulgida*, an ammonium oxidising and nitrite reducing
326 microorganism (77). In general, given the large range of substrates utilized by the CISM
327 superfamily and the few biochemically characterized proteins, the predicted function of all
328 those annotated in the *Methanoperedenaceae* require empirical verification. Nonetheless, the

329 range of putative CISM superfamily proteins encoded by members of the family likely
330 indicates diverse respiratory strategies that remain to be characterised.

331

332 *The diversity of the MHCs in the Methanoperedenaceae*

333 Members of the *Methanoperedenaceae* possess a diverse repertoire of MHCs which have
334 been suggested to facilitate the transfer of electrons from the re-oxidation of MK to metal
335 oxides (9, 10, 78) or direct interspecies electron transfer (DIET) to a syntrophic partner.
336 Analyses of the *Methanoperedenaceae* revealed that they possess between three (MGW-1)
337 and 49 (IPS-1) MHCs (containing at least three CXXCH motifs) with an average of 26 – the
338 highest average of any archaeal family (**Dataset S1F and S1G**). Notably, relatively high
339 numbers of MHCs per genome are almost exclusively found in microorganisms associated
340 with DIET, metal and/or sulfur reduction, such as the *Geobacteraceae* (79) (≤ 87 MHCs),
341 *Shewanellaceae* (80) (≤ 63 MHCs), *Desulfurivibrionaceae* (20), *Desulfuromonadaceae* (20)
342 and *Defferisomataceae* (81) (≤ 50 MHCs; **Dataset S1G**). Interestingly, seven of the 16
343 members of the *Methanoperedenaceae* encode MHCs with more than 50 heme binding sites
344 (ASW-5, ASW-6, BLZ2, HGW-1, M. ferri, Mn-1 and Mn-2), with the 113 heme MHC
345 encoded by Mn-2 the largest identified in any microorganism (**Dataset S1F**).

346 The 414 putative MHCs identified in the *Methanoperedenaceae* MAGs clustered into 82
347 orthologous protein families (**Figure S8**). Only one protein family (OG0000252) included at
348 least one MHC from each member, which suggests low conservation of these genes within
349 the *Methanoperedenaceae*. Out of the 82 MHC protein families, 14 were identified in at least
350 eight of the 16 MAGs, with five of these found within the conserved MK:cytochrome *c*
351 oxidoreductase clusters. A lack of conservation of MHCs is also observed for the anaerobic
352 metal-respiring genus *Geobacter*, where 14% of the MHCs encoded in six analysed genomes

353 were found to be conserved (61). Thirty-nine of the 82 MHC protein families had significant
354 hits ($1e-20$, $\geq 50\%$ AAI) to homologs from diverse lineages across the bacterial and archaeal
355 domains in the GTDB89 database, indicating potential LGT of these genes (**Figure S9**).
356 These lineages notably included the metal reducing *Geobacteraceae* and *Shewanellaceae*,
357 along with the alkane oxidising *Archaeoglobaceae*, Methylospirillum (NC10), and other
358 ANME-lineages (**Figure S9**).

359

360 *Putative function of MHCs in the Methanoperedenaceae*

361 Very few of the *Methanoperedenaceae* MHCs could be associated with a specific function.
362 Two orthologous groups were annotated as nitrite: ammonium oxidoreductases (NrfA) with
363 homologs identified in bacterial MAGs classified to the Anaerolineales (OG0004545; $\geq 66.3\%$
364 AAI) and the candidate phylum UBP4 (OG0012490, 64.56% AAI). Several MHCs were also
365 identified as part of the MK:cytochrome *c* oxidoreductase clusters, with homologs observed
366 in members of the archaeal family *Archaeoglobaceae* (OG001557, OG000137, OG0001550,
367 $\geq 57.3\%$ AAI; **Figure S9**). MHC/S-layer fusion proteins were suggested to mediate the
368 transfer of electrons across the S-layer for marine ANME-2 (ref. 7) and were relatively highly
369 expressed by ‘*Ca. M. manganicus*’ and ‘*Ca. M. manganireducens*’ during AOM coupled to
370 Mn(IV) reduction (12). Conversely, only low expression of MHC/S-layer protein genes
371 encoded by ‘*Ca. M. ferrireducens*’ was observed during AOM coupled to Fe(III) reduction
372 (9). In addition, despite all the *Methanoperedenaceae* MAGs containing S-layer proteins, five
373 do not encode MHC proteins with an S-layer domain (ASW-3, CMD-1, CMD-2, HGW-1 and
374 MGW-1), indicating alternative mechanisms for electron transfer across the S-layer to
375 extracellular MHCs for these species.

376 Predicted extracellular MHCs are hypothesized to facilitate the final transfer of electrons
377 from the *Methanoperedenaceae* to metal oxides (9). Interestingly, ‘*Ca. M. manganicus*’ and
378 ‘*Ca. M. manganireducens*’ showed differential expression patterns in the complement of
379 shared extracellular MHCs during AOM coupled to Mn(IV) reduction. In addition, no
380 orthologs for the two MHCs highly transcribed by ‘*Ca. M. ferrireducens*’ during AOM
381 coupled to Fe(III) reduction (9) were identified in other members of the
382 *Methanoperedenaceae* (OG0011636 and OG0003254; **Figure S8**), suggesting that BLZ2
383 utilises a different MHC for iron reduction linked to AOM (10). These observations suggest
384 that the *Methanoperedenaceae* can utilise multiple mechanisms for the reduction of similar
385 metal oxides. Differential expression of conserved MHCs linked to extracellular electron
386 transfer was also observed for different *Geobacteraceae* species enriched on electrodes when
387 exposed to the same surface redox potential (82). As suggested for members of the
388 *Geobacteraceae*, the large MHC repertoire possessed by the *Methanoperedenaceae* may
389 enable adaptation to the use of a range of terminal electron acceptors.

390 This study has substantially improved the genome coverage of the *Methanoperedenaceae*.
391 Comparative genomic analysis of this lineage highlights a metabolic plasticity not found in
392 other ANME clades. The subsequent ability of members of the family to adapt to the use of
393 terminal electron acceptors across a range of redox potentials likely contributes to their
394 success in diverse environments (**Table 1**). Notably, based on the genome tree (**Figure 1**),
395 and the lack of conservation of MHCs (**Figure S8**), the acquisition of these genes is not
396 congruent with the genome-based phylogeny of the family, suggesting niche specific
397 adaptations as the main driver for these LGT events. While further studies are necessary to
398 verify the general physiology and energy conservation mechanisms of the
399 *Methanoperedenaceae* in different environments, this study provides genomic evidence that
400 members of the family may play key roles in coupling cycling of carbon with selenate, sulfur,

401 and arsenic in addition to nitrogen and metal oxides. Continued sequencing and
402 characterisation of this lineage will reveal the full extent of their metabolic versatility and
403 influence on global biogeochemical cycles.

404

405 **Materials and Methods**

406 *Recovery of the genomes from SRA*

407 The NCBI sequence read archive (SRA (83)) was accessed on the 22nd of March 2017 and
408 14516 datasets classified as environmental metagenomes were downloaded. The
409 metagenomic datasets were screened using GraftM (32) to search for 16S rRNA and *mcrA*
410 gene sequences similar to those from members of the *Methanoperedenaceae*. For datasets
411 where members of the family were detected, all paired-end read sets were trimmed and
412 quality filtered using PEAT v1.2.4 (ref. 84). For genomes, CMD-1 and CMD-2, SRR5161805
413 and SRR5161795 reads were coassembled using Metaspades, version 3.10.0 using the default
414 parameters (85). For the ASW genomes, SRR1563167, SRR1564103, SRR1573565, and
415 SRR1573578 reads were coassembled using Metaspades, version 3.10.0 with default
416 parameters (85). Mapping of quality reads was performed using BamM v1.7.3 with default
417 parameters (<https://github.com/CoGenomics/BamM>). Metagenomic assembled genomes
418 were recovered from the assembled metagenomes using uniteM v0.0.14
419 (<https://github.com/dparks1134/UniteM>). The *Methanoperedenaceae* MAGs were further
420 refined by reassembling the mapped quality trimmed reads with SPAdes using the `–careful`
421 and `–trusted-contigs` setting. Additional scaffolding and resolving ambiguous bases of the
422 MAGs was performed using the ‘roundup’ mode of FinishM v0.0.7
423 (<https://github.com/wwood/finishm>). Completeness and contamination rates of the population
424 bins were assessed using CheckM v1.0.11 (ref. 33) with the ‘lineage wf’ command. The

425 genomes assembled in this study have been deposited in NCBI under the accession numbers
426 SAMN10961276- SAMN10961283.

427

428 *Functional annotation*

429 For all MAGs, open reading frames (ORF) were called and annotated using Prokka v.1.12
430 (ref. 86). Additional annotation was performed using the blastp ‘verysensitive’ setting in
431 Diamond v0.9.18 (<https://github.com/bbuchfink/diamond.git>) against UniRef100 (accessed
432 September 2017) (87), clusters of orthologous groups (COG) (88), Pfam 31 (ref. 89) and
433 TIGRfam (Release: January 2014) (90). ORFs were also diamond blastp searched against
434 Uniref100 (accessed September 2017) containing proteins with KO ID. The top hit for each
435 gene with an e-value $<1e^{-3}$ was mapped to the KO database (91) using the Uniprot ID
436 mapping files. Genes of interest were further verified using NCBI’s conserved domain search
437 to identify conserved motif(s) present within the gene (92). Psortb v3.0 (ref. 93) was used to
438 predict subcellular localisation of the putative proteins. Pred-Tat was used to predict putative
439 signal peptides (94). Putative multi-heme *c*-type cytochromes (MHCs) were identified by
440 ORFs possessing ≥ 3 CXXCH motifs. Putative MHCs were subsequently searched for
441 cytochrome *c*-type protein domains using hmmsearch (HMMER v.3.1) (95) with PfamA (96).

442

443 *Construction of genome trees*

444 The archaeal genome tree was constructed using GTDB-Tk (GTDBtk v0.2.2,
445 <https://github.com/Ecogenomics/GTDBTk/releases>) with a concatenated set of 122 archaeal-
446 specific conserved marker genes inferred from genomes available in NCBI (NCBI RefSeq
447 release 83) (34). Marker genes were identified and aligned in each genome using HMMER
448 v.3.1 (ref. 95), concatenated, and trees were constructed using FastTree V.2.1.8 (ref. 97) with

449 the WAG+GAMMA models. Support values were determined using 100 nonparametric
450 bootstrapping with GenomeTreeTK. The trees were visualised using ARB (98) and formatted
451 using Adobe Illustrator (Adobe, USA).

452

453 *Construction of 16S rRNA gene tree*

454 The 16S rRNA gene was identified in MAGs and used to infer taxonomic assignment of the
455 population genome implementing the SILVA 16S rRNA gene database (Version 132).
456 Sequences were aligned with 426 16S rRNA gene sequences retrieved from the SILVA
457 database using SSU-align v0.1 (ref. 99). The phylogenetic tree was constructed using
458 FastTree V2.1.8 (ref. 97) with the Generalised Time-Reversible and GAMMA model.
459 Support values were determined using 100 nonparametric bootstrapping. The trees were
460 visualised using ARB (98) and formatted using Adobe Illustrator.

461

462 *Calculation of amino acid identity*

463 The *Methanoperedenaceae* MAGs identified in this study were compared to publicly
464 available genomes of the family. Average amino acid identity (AAI) between the genomes
465 was calculated using orthologous genes identified through reciprocal best BLAST hits using
466 compareM v0.0.5 (<https://github.com/dparks1134/CompareM>).

467

468 *Identification of orthologous proteins*

469 Homologous proteins across all the *Methanoperedenaceae*, GoM-Arc I, ANME-2a, ANME-2c
470 MAGs were identified with OrthoFinder (100) v2.3.3 using default parameters. Gene counts
471 of orthologous groups containing MHCs were used as input for a heatmap using the
472 pheatmap package in R and hierarchical clustering was performed using ward.D2 (ref. 101).

473

474 *Construction of gene trees*

475 Genes of interest in the *Methanoperedenaceae* MAGs were compared against proteins from
476 GTDB v83 database (34) using the genetreetk ‘blast’ command to identify closely related
477 sequences. For the generation of the gene tree for catalytic subunits of the CISM superfamily,
478 curated protein sequences were also added in the analysis. Accession numbers and amino
479 acid sequences are included in **Dataset S1B**. For the generation of the gene tree for the
480 catalytic subunits of the Group 1 and Group 3 NiFe dehydrogenase, curated sequences from
481 Greening *et al.*, (102) were included in the analysis. Accession numbers and amino acid
482 sequences can be found in **Dataset S1C**. The sequences were subsequently aligned using
483 mafft v7.221 (ref. 103) with the –auto function and the alignment trimmed using trimal v1.2
484 (<https://github.com/scapella/trimal>) ‘-automated1’ option. A phylogenetic tree was
485 constructed using RAxML v8.2.9 (ref. 104) with the following parameters: raxmlHPC-
486 PTHREADS-SSE3 -T 30 -m PROTGAMMALG -p 12345. Bootstrap values were calculated
487 via non-parametric bootstrapping with 100 replicates. The trees were visualised using ARB
488 (98) or iTOL (105) and formatted using Adobe Illustrator (Adobe, USA).

489

490 *Network analysis of MHCs*

491 Putative multi-heme *c*-type cytochromes (MHCs) from GTDB v89 database were identified
492 by ORFs possessing ≥ 3 CXXCH. Putative MHCs were subsequently searched for
493 cytochrome *c*-type protein domains using hmmsearch (HMMER v.3.1) (95) with PfamA (96).
494 Proteins from each *Methanoperedenaceae* orthogroup were blasted against the GTDB v89
495 MHC protein database using DIAMOND with an evalue cutoff of $1e-20$ and $\geq 50\%$ AAI. The

496 result was visualised in Cytoscape v3.7.1, removing clusters that contained only, or no,
497 *Methanoperedenaceae* homologs.

498

499 **Acknowledgements**

500 This work was supported by the Australian Research Council (ARC) (FT170100070) and the
501 U.S. Department of Energy’s Office of Biological Environmental Research (DE-SC0016469).
502 AOL was supported by an ARC Australian Postgraduate Award. We thank the AWMC team,
503 particularly Shihu Hu and Zhiguo Yuan, for their ongoing collaboration working on various
504 “*Ca. Methanoperedens*” enrichments.

505

506 **Competing interests**

507 The authors have nothing to disclose.

508

509

510 **References**

511

512 1. Reeburgh WS. Oceanic methane biogeochemistry. *Chemical Reviews*.

513 2007;107(2):486-513.

514 2. Segarra K, Schubotz F, Samarkin V, Yoshinaga M, Hinrichs K, Joye S. High rates of

515 anaerobic methane oxidation in freshwater wetlands reduce potential atmospheric methane

516 emissions. *Nature Communications*. 2015;6:7477.

517 3. Martinez-Cruz K, Sepulveda-Jauregui A, Casper P, Anthony KW, Smemo KA,

518 Thalasso F. Ubiquitous and significant anaerobic oxidation of methane in freshwater lake

519 sediments. *Water Research*. 2018;144:332-40.

520 4. Thamdrup B, Steinsdottir HGR, Bertagnolli A, Padilla C, Patin NV, Garcia-Robledo

521 E, et al. Anaerobic methane oxidation is an important sink for methane in the ocean's largest

522 oxygen minimum zone. *Limnol Oceanogr*. 2019;64(6):2569-85.

523 5. Ettwig KF, Butler MK, Le Paslier D, Pelletier E, Mangenot S, Kuypers MM, et al.

524 Nitrite-driven anaerobic methane oxidation by oxygenic bacteria. *Nature*.

525 2010;464(7288):543-8.

526 6. McGlynn SE. Energy Metabolism during Anaerobic Methane Oxidation in ANME

527 Archaea. *Microbes and Environments*. 2017;32(1):5-13.

528 7. McGlynn SE, Chadwick GL, Kempes CP, Orphan VJ. Single cell activity reveals

529 direct electron transfer in methanotrophic consortia. *Nature*. 2015;526:531-5.

530 8. Wegener G, Krukenberg V, Riedel D, Tegetmeyer HE, Boetius A. Intercellular wiring

531 enables electron transfer between methanotrophic archaea and bacteria. *Nature*.

532 2015;526(7574):587-90.

533 9. Cai C, Leu AO, Xie G-J, Guo J, Feng Y, Zhao J-X, et al. A methanotrophic archaeon

534 couples anaerobic oxidation of methane to Fe (III) reduction. *The ISME Journal*.

535 2018;12:1929-39.

- 536 10. Ettwig KF, Zhu B, Speth D, Keltjens JT, Jetten MSM, Kartal B. Archaea catalyze
537 iron-dependent anaerobic oxidation of methane. *Proceedings of the National Academy of*
538 *Sciences*. 2016;45:12792-6.
- 539 11. Scheller S, Yu H, Chadwick GL, McGlynn SE, Orphan VJ. Artificial electron
540 acceptors decouple archaeal methane oxidation from sulfate reduction. *Science*.
541 2016;351(6274):703-7.
- 542 12. Leu AO, Cai C, McIlroy SJ, Southam G, Orphan VJ, Yuan Z, et al. Anaerobic
543 methane oxidation coupled to manganese reduction by members of the
544 *Methanoperedenaceae*. *ISME J*. 2020;<https://doi.org/10.1038/s41396-020-0590-x>.
- 545 13. Knittel K, Lösekann T, Boetius A, Kort R, Amann R. Diversity and distribution of
546 methanotrophic archaea at cold seeps. *Applied and Environmental Microbiology*.
547 2005;71(1):467-79.
- 548 14. Orphan VJ, House CH, Hinrichs K-U, McKeegan KD, DeLong EF. Multiple archaeal
549 groups mediate methane oxidation in anoxic cold seep sediments. *Proceedings of the*
550 *National Academy of Sciences*. 2002;99(11):7663-8.
- 551 15. Haroon MF, Hu S, Shi Y, Imelfort M, Keller J, Hugenholtz P, et al. Anaerobic
552 oxidation of methane coupled to nitrate reduction in a novel archaeal lineage. *Nature*.
553 2013;500(7464):567-70.
- 554 16. Orphan V, Hinrichs K-U, Ussler W, Paull CK, Taylor L, Sylva SP, et al. Comparative
555 analysis of methane-oxidizing archaea and sulfate-reducing bacteria in anoxic marine
556 sediments. *Appl Environ Microbiol*. 2001;67(4):1922-34.
- 557 17. Pernthaler A, Dekas AE, Brown CT, Goffredi SK, Embaye T, Orphan VJ. Diverse
558 syntrophic partnerships from deep-sea methane vents revealed by direct cell capture and
559 metagenomics. *Proceedings of the National Academy of Sciences*. 2008;105(19):7052-7.

- 560 18. Hatzenpichler R, Connon SA, Goudeau D, Malmstrom RR, Woyke T, Orphan VJ.
561 Visualizing in situ translational activity for identifying and sorting slow-growing archaeal-
562 bacterial consortia. *Proceedings of the National Academy of Sciences*. 2016;113(28):E4069-
563 E78.
- 564 19. Schreiber L, Holler T, Knittel K, Meyerdierks A, Amann R. Identification of the
565 dominant sulfate-reducing bacterial partner of anaerobic methanotrophs of the ANME-2
566 clade. *Environmental Microbiology*. 2010;12(8):2327-40.
- 567 20. Skennerton CT, Chourey K, Iyer R, Hettich RL, Tyson GW, Orphan VJ. Methane-
568 fueled syntrophy through extracellular electron transfer: uncovering the genomic traits
569 conserved within diverse bacterial partners of anaerobic methanotrophic archaea. *MBio*.
570 2017;8(4):e00530-17.
- 571 21. Holler T, Widdel F, Knittel K, Amann R, Kellermann MY, Hinrichs K-U, et al.
572 Thermophilic anaerobic oxidation of methane by marine microbial consortia. *The ISME*
573 *journal*. 2011;5(12):1946.
- 574 22. Niemann H, Lösekann T, De Beer D, Elvert M, Nadalig T, Knittel K, et al. Novel
575 microbial communities of the Haakon Mosby mud volcano and their role as a methane sink.
576 *Nature*. 2006;443(7113):854.
- 577 23. Su GY, Zopfi J, Yao HY, Steinle L, Niemann H, Lehmann MF. Manganese/iron-
578 supported sulfate-dependent anaerobic oxidation of methane by archaea in lake sediments.
579 *Limnol Oceanogr*. 2019.
- 580 24. Arshad A, Speth DR, de Graaf RM, den Camp HJO, Jetten MS, Welte CU. A
581 Metagenomics-Based Metabolic Model of Nitrate-Dependent Anaerobic Oxidation of
582 Methane by Methanoperedens-Like Archaea. *Frontiers in Microbiology*. 2015;6.
- 583 25. Lu Y-Z, Fu L, Ding J, Ding Z-W, Li N, Zeng RJ. Cr (VI) reduction coupled with
584 anaerobic oxidation of methane in a laboratory reactor. *Water Research*. 2016;102:445-52.

- 585 26. Luo J-H, Chen H, Hu S, Cai C, Yuan Z, Guo J. Microbial selenate reduction driven by
586 a denitrifying anaerobic methane oxidation biofilm. *Environmental Science and Technology*.
587 2018;52(7):4006-12.
- 588 27. Shen LD, Ouyang L, Zhu YZ, Trimmer M. Active pathways of anaerobic methane
589 oxidation across contrasting riverbeds. *ISME Journal*. 2019;13(3):752-66.
- 590 28. Berger S, Frank J, Martins PD, Jetten MS, Welte CU. High-quality draft genome
591 sequence of “*Candidatus Methanoperedens* sp.” strain BLZ2, a nitrate-reducing anaerobic
592 methane-oxidizing archaeon enriched in an anoxic bioreactor. *Genome Announcements*.
593 2017;5(46):e01159-17.
- 594 29. Ino K, Hermsdorf AW, Konno U, Kouduka M, Yanagawa K, Kato S, et al. Ecological
595 and genomic profiling of anaerobic methane-oxidizing archaea in a deep granitic
596 environment. *The ISME journal*. 2017;12(1):31.
- 597 30. Hermsdorf AW, Amano Y, Miyakawa K, Ise K, Suzuki Y, Anantharaman K, et al.
598 Potential for microbial H₂ and metal transformations associated with novel bacteria and
599 archaea in deep terrestrial subsurface sediments. *The ISME journal*. 2017;11(8):1915.
- 600 31. Vaksmaa A, Lüke C, Van Alen T, Vale G, Lupotto E, Jetten M, et al. Distribution and
601 activity of the anaerobic methanotrophic community in a nitrogen-fertilized Italian paddy
602 soil. *FEMS Microbiology Ecology*. 2016;92(12).
- 603 32. Boyd JA, Woodcroft BJ, Tyson GW. GraftM: a tool for scalable, phylogenetically
604 informed classification of genes within metagenomes. *Nucleic Acids Research*. 2018.
- 605 33. Parks DH, Imelfort M, Skennerton CT, Hugenholtz P, Tyson GW. CheckM: assessing
606 the quality of microbial genomes recovered from isolates, single cells, and metagenomes.
607 *Genome research*. 2015;25(7):1043-55.

- 608 34. Parks DH, Chuvochina M, Waite DW, Rinke C, Skarszewski A, Chaumeil P-A, et al.
609 A standardized bacterial taxonomy based on genome phylogeny substantially revises the tree
610 of life. *Nature biotechnology*. 2018.
- 611 35. Konstantinidis KT, Tiedje JM. Towards a genome-based taxonomy for prokaryotes.
612 *Journal of Bacteriology*. 2005;187(18):6258-64.
- 613 36. Thauer RK, Jungermann K, Decker K. Energy conservation in chemotrophic
614 anaerobic bacteria. *Bacteriological Reviews*. 1977;41(1):100.
- 615 37. Nauhaus K, Treude T, Boetius A, Kruger M. Environmental regulation of the
616 anaerobic oxidation of methane: a comparison of ANME-I and ANME-II communities.
617 *Environ Microbiol*. 2005;7(1):98-106.
- 618 38. Meyerdierks A, Kube M, Kostadinov I, Teeling H, Glockner FO, Reinhardt R, et al.
619 Metagenome and mRNA expression analyses of anaerobic methanotrophic archaea of the
620 ANME-1 group. *Environ Microbiol*. 2010;12(2):422-39.
- 621 39. Loach PA. Oxidation-reduction potentials, absorbance bands and molar absorbance of
622 compounds used in biochemical studies. *Handbook of Biochemistry and Molecular Biology*.
623 1976;1:122-30.
- 624 40. Jungbluth SP, Amend JP, Rappé MS. Metagenome sequencing and 98 microbial
625 genomes from Juan de Fuca Ridge flank subsurface fluids. *Scientific Data*. 2017;4:170037.
- 626 41. Welte C, Deppenmeier U. Bioenergetics and anaerobic respiratory chains of
627 acetoclastic methanogens. *Biochimica et Biophysica Acta (BBA)-Bioenergetics*.
628 2014;1837(7):1130-47.
- 629 42. Kanai T, Matsuoka R, Beppu H, Nakajima A, Okada Y, Atomi H, et al. Distinct
630 physiological roles of the three [NiFe]-hydrogenase orthologs in the hyperthermophilic
631 archaeon *Thermococcus kodakarensis*. *Journal of Bacteriology*. 2011;193(12):3109-16.

- 632 43. Ma K, Schicho RN, Kelly RM, Adams M. Hydrogenase of the hyperthermophile
633 *Pyrococcus furiosus* is an elemental sulfur reductase or sulfhydrogenase: evidence for a
634 sulfur-reducing hydrogenase ancestor. *Proceedings of the National Academy of Sciences*.
635 1993;90(11):5341-4.
- 636 44. Berney M, Greening C, Hards K, Collins D, Cook GM. Three different [NiFe]
637 hydrogenases confer metabolic flexibility in the obligate aerobe *Mycobacterium smegmatis*.
638 *Environmental Microbiology*. 2014;16(1):318-30.
- 639 45. Stanley EH, Casson NJ, Christel ST, Crawford JT, Loken LC, Oliver SK. The
640 ecology of methane in streams and rivers: patterns, controls, and global significance. *Ecol*
641 *Monogr*. 2016;86(2):146-71.
- 642 46. Deppenmeier U, Blaut M, Mahlmann A, Gottschalk G. Reduced coenzyme F420:
643 heterodisulfide oxidoreductase, a proton-translocating redox system in methanogenic
644 bacteria. *Proceedings of the National Academy of Sciences*. 1990;87(23):9449-53.
- 645 47. Timmers PH, Welte CU, Koehorst JJ, Plugge CM, Jetten MS, Stams AJ. Reverse
646 methanogenesis and respiration in methanotrophic archaea. *Archaea*. 2017;2017:1654237.
- 647 48. Walsh C. Naturally occurring 5-deazaflavin coenzymes: biological redox roles.
648 *Accounts of Chemical Research*. 1986;19(7):216-21.
- 649 49. Tran QH, Uden G. Changes in the proton potential and the cellular energetics of
650 *Escherichia coli* during growth by aerobic and anaerobic respiration or by fermentation.
651 *European Journal of Biochemistry*. 1998;251(1-2):538-43.
- 652 50. Tietze M, Beuchle A, Lamla I, Orth N, Dehler M, Greiner G, et al. Redox potentials
653 of methanophenazine and CoB-S-S-CoM, factors involved in electron transport in
654 methanogenic archaea. *Chembiochem*. 2003;4(4):333-5.

- 655 51. Gonzalez O, Gronau S, Pfeiffer F, Mendoza E, Zimmer R, Oesterhelt D. Systems
656 analysis of bioenergetics and growth of the extreme halophile *Halobacterium salinarum*.
657 PLoS Comput Biol. 2009;5(4):e1000332.
- 658 52. Jones AJ, Blaza JN, Varghese F, Hirst J. Respiratory complex I in *Bos taurus* and
659 *Paracoccus denitrificans* pumps four protons across the membrane for every NADH oxidized.
660 Journal of Biological Chemistry. 2017;12:4987-95.
- 661 53. Sazanov LA. A giant molecular proton pump: structure and mechanism of respiratory
662 complex I. Nature Reviews Molecular Cell Biology. 2015;16(6):375.
- 663 54. Dombrowski N, Seitz KW, Teske AP, Baker BJ. Genomic insights into potential
664 interdependencies in microbial hydrocarbon and nutrient cycling in hydrothermal sediments.
665 Microbiome. 2017;5(1):106.
- 666 55. Borrel G, Adam PS, McKay LJ, Chen L-X, Sierra-García IN, Sieber CM, et al. Wide
667 diversity of methane and short-chain alkane metabolisms in uncultured archaea. Nature
668 Microbiology. 2019:1.
- 669 56. Wang FP, Zhang Y, Chen Y, He Y, Qi J, Hinrichs KU, et al. Methanotrophic archaea
670 possessing diverging methane-oxidizing and electron-transporting pathways. ISME J.
671 2014;8(5):1069-78.
- 672 57. Schlegel K, Muller V. Evolution of Na and H bioenergetics in methanogenic archaea.
673 Biochem Soc Trans. 2013;41:421-6.
- 674 58. Schlegel K, Welte C, Deppenmeier U, Müller V. Electron transport during acetoclastic
675 methanogenesis by *Methanosarcina acetivorans* involves a sodium-translocating Rnf
676 complex. The FEBS journal. 2012;279(24):4444-52.
- 677 59. Welte C, Deppenmeier U. Membrane-bound electron transport in *Methanosarcina*
678 *thermophila*. Journal of Bacteriology. 2011;193(11):2868-70.

- 679 60. Anderson I, Risso C, Holmes D, Lucas S, Copeland A, Lapidus A, et al. Complete
680 genome sequence of *Ferroglobus placidus* AEDII12DO. *Standards in genomic sciences*.
681 2011;5(1):50.
- 682 61. Butler JE, Young ND, Lovley DR. Evolution of electron transfer out of the cell:
683 comparative genomics of six *Geobacter* genomes. *BMC Genomics*. 2010;11(1):40.
- 684 62. Mardanov AV, Slododkina GB, Slobodkin AI, Beletsky AV, Gavrilov SN, Kublanov
685 IV, et al. The *Geoglobus acetivorans* genome: Fe (III) reduction, acetate utilization,
686 autotrophic growth, and degradation of aromatic compounds in a hyperthermophilic
687 archaeon. *Applied and environmental microbiology*. 2015;81(3):1003-12.
- 688 63. Straub KL, Schink B. Ferrihydrite reduction by *Geobacter* species is stimulated by
689 secondary bacteria. *Archives of Microbiology*. 2004;182(2-3):175-81.
- 690 64. Levar CE, Hoffman CL, Dunshee AJ, Toner BM, Bond DR. Redox potential as a
691 master variable controlling pathways of metal reduction by *Geobacter sulfurreducens*. *The*
692 *ISME Journal*. 2017;11:741-52.
- 693 65. Vaksmaa A, Guerrero-Cruz S, van Alen TA, Cremers G, Ettwig KF, Lüke C, et al.
694 Enrichment of anaerobic nitrate-dependent methanotrophic ‘*Candidatus Methanoperedens*
695 *nitroreducens*’ archaea from an Italian paddy field soil. *Applied Microbiology and*
696 *Biotechnology*. 2017;101(18):7075-84.
- 697 66. Guiral M, Tron P, Aubert C, Gloter A, Iobbi-Nivol C, Giudici-Orticoni M-T. A
698 membrane-bound multienzyme, hydrogen-oxidizing, and sulfur-reducing complex from the
699 hyperthermophilic bacterium *Aquifex aeolicus*. *Journal of Biological Chemistry*.
700 2005;280(51):42004-15.
- 701 67. Vigneron A, Alsop EB, Cruaud P, Philibert G, King B, Baksmaty L, et al. Contrasting
702 Pathways for Anaerobic Methane Oxidation in Gulf of Mexico Cold Seep Sediments.
703 *Msystems*. 2019;4(1).

- 704 68. Yu H, Susanti D, McGlynn SE, Skennerton CT, Chourey K, Iyer R, et al.
705 Comparative Genomics and Proteomic Analysis of Assimilatory Sulfate Reduction Pathways
706 in Anaerobic Methanotrophic Archaea. *Frontiers in Microbiology*. 2018;9.
- 707 69. Zargar K, Conrad A, Bernick DL, Lowe TM, Stolc V, Hoefft S, et al. ArxA, a new
708 clade of arsenite oxidase within the DMSO reductase family of molybdenum
709 oxidoreductases. *Environmental Microbiology*. 2012;14(7):1635-45.
- 710 70. Takami H, Noguchi H, Takaki Y, Uchiyama I, Toyoda A, Nishi S, et al. A deeply
711 branching thermophilic bacterium with an ancient acetyl-CoA pathway dominates a
712 subsurface ecosystem. *Plos One*. 2012;7(1):e30559.
- 713 71. Nordstrom DK. Worldwide occurrences of arsenic in ground water. *Science*.
714 2002;296:2143-5.
- 715 72. Smedley PL, Kinniburgh D. A review of the source, behaviour and distribution of
716 arsenic in natural waters. *Applied Geochemistry*. 2002;17(5):517-68.
- 717 73. Council NR. *Arsenic in drinking water*: National Academies Press; 1999.
- 718 74. Harvey CF, Swartz CH, Badruzzaman ABM, Keon-Blute N, Yu W, Ali MA, et al.
719 Arsenic mobility and groundwater extraction in Bangladesh. *Science*. 2002;298(5598):1602-
720 6.
- 721 75. Polizzotto ML, Harvey CF, Sutton SR, Fendorf S. Processes conducive to the release
722 and transport of arsenic into aquifers of Bangladesh. *P Natl Acad Sci USA*.
723 2005;102(52):18819-23.
- 724 76. Anantharaman K, Brown CT, Hug LA, Sharon I, Castelle CJ, Probst AJ, et al.
725 Thousands of microbial genomes shed light on interconnected biogeochemical processes in
726 an aquifer system. *Nature Communications*. 2016;7:13219.

- 727 77. Gori F, Tringe SG, Kartal B, Machiori E, Jetten MS. The metagenomic basis of
728 anammox metabolism in Candidatus 'Brocadia fulgida'. *Biochem Soc Trans.* 2011;39:1799-
729 804.
- 730 78. Kletzin A, Heimerl T, Flechsler J, van Niftrik L, Rachel R, Klingl A. Cytochromes c
731 in Archaea: distribution, maturation, cell architecture, and the special case of *Ignicoccus*
732 *hospitalis*. *Frontiers in microbiology.* 2015;6:439.
- 733 79. Methé B, Nelson KE, Eisen JA, Paulsen IT, Nelson W, Heidelberg J, et al. Genome of
734 *Geobacter sulfurreducens*: metal reduction in subsurface environments. *Science.*
735 2003;302(5652):1967-9.
- 736 80. Heidelberg JF, Paulsen IT, Nelson KE, Gaidos EJ, Nelson WC, Read TD, et al.
737 Genome sequence of the dissimilatory metal ion-reducing bacterium *Shewanella oneidensis*.
738 *Nature Biotechnology.* 2002;20(11):1118.
- 739 81. Slobodkina G, Reysenbach A-L, Panteleeva A, Kostrikina N, Wagner I, Bonch-
740 Osmolovskaya E, et al. *Deferrisoma camini* gen. nov., sp. nov., a moderately thermophilic,
741 dissimilatory iron (III)-reducing bacterium from a deep-sea hydrothermal vent that forms a
742 distinct phylogenetic branch in the Deltaproteobacteria. *International Journal of Systematic*
743 *Evolutionary Microbiology.* 2012;62(10):2463-8.
- 744 82. Ishii Si, Suzuki S, Tenney A, Nealson KH, Bretschger O. Comparative
745 metatranscriptomics reveals extracellular electron transfer pathways conferring microbial
746 adaptivity to surface redox potential changes. *The ISME journal.* 2018;12(12):2844.
- 747 83. Cochrane G, Karsch-Mizrachi I, Takagi T, Sequence Database Collaboration IN. The
748 international nucleotide sequence database collaboration. *Nucleic Acids Research.*
749 2015;44(D1):D48-D50.

- 750 84. Li Y-L, Weng J-C, Hsiao C-C, Chou M-T, Tseng C-W, Hung J-H, editors. PEAT: an
751 intelligent and efficient paired-end sequencing adapter trimming algorithm. *BMC*
752 *Bioinformatics*; 2015: BioMed Central.
- 753 85. Nurk S, Meleshko D, Korobeynikov A, Pevzner PA. metaSPAdes: a new versatile
754 metagenomic assembler. *Genome Research*. 2017;gr. 213959.116.
- 755 86. Seemann T. Prokka: rapid prokaryotic genome annotation. *Bioinformatics*.
756 2014;30(14):2068-9.
- 757 87. Suzek BE, Huang H, McGarvey P, Mazumder R, Wu CH. UniRef: comprehensive
758 and non-redundant UniProt reference clusters. *Bioinformatics*. 2007;23(10):1282-8.
- 759 88. Tatusov RL, Fedorova ND, Jackson JD, Jacobs AR, Kiryutin B, Koonin EV, et al.
760 The COG database: an updated version includes eukaryotes. *BMC Bioinformatics*.
761 2003;4(1):41.
- 762 89. Finn RD, Coghill P, Eberhardt RY, Eddy SR, Mistry J, Mitchell AL, et al. The Pfam
763 protein families database: towards a more sustainable future. *Nucleic Acids Research*.
764 2016;44(D1):D279-D85.
- 765 90. Haft DH, Selengut JD, Richter RA, Harkins D, Basu MK, Beck E. TIGRFAMs and
766 genome properties in 2013. *Nucleic Acids Research*. 2013;41(D1):D387-D95.
- 767 91. Burns JL, Ginn BR, Bates DJ, Dublin SN, Taylor JV, Apkarian RP, et al. Outer
768 membrane-associated serine protease involved in adhesion of *Shewanella oneidensis* to Fe
769 (III) oxides. *Environ Sci Technol*. 2009;44(1):68-73.
- 770 92. Marchler-Bauer A, Bryant SH. CD-Search: protein domain annotations on the fly.
771 *Nucleic Acids Research*. 2004;32(suppl 2):W327-W31.
- 772 93. Yu NY, Wagner JR, Laird MR, Melli G, Rey S, Lo R, et al. PSORTb 3.0: improved
773 protein subcellular localization prediction with refined localization subcategories and
774 predictive capabilities for all prokaryotes. *Bioinformatics*. 2010;26(13):1608-15.

- 775 94. Bagos PG, Nikolaou EP, Liakopoulos TD, Tsirigos KD. Combined prediction of Tat
776 and Sec signal peptides with hidden Markov models. *Bioinformatics*. 2010;26(22):2811-7.
- 777 95. Eddy SR. Accelerated profile HMM searches. *PLoS Comput Biol*.
778 2011;7(10):e1002195.
- 779 96. Bateman A, Coin L, Durbin R, Finn RD, Hollich V, Griffiths-Jones S, et al. The Pfam
780 protein families database. *Nucleic Acids Research*. 2004;32(suppl 1):D138-D41.
- 781 97. Price MN, Dehal PS, Arkin AP. FastTree 2—approximately maximum-likelihood trees
782 for large alignments. *Plos One*. 2010;5(3):e9490.
- 783 98. Ludwig W, Strunk O, Westram R, Richter L, Meier H, Buchner A, et al. ARB: a
784 software environment for sequence data. *Nucleic Acids Research*. 2004;32(4):1363-71.
- 785 99. Nawrocki EP, Kolbe DL, Eddy SR. Infernal 1.0: inference of RNA alignments.
786 *Bioinformatics*. 2009;25(10):1335-7.
- 787 100. Emms DM, Kelly S. OrthoFinder: solving fundamental biases in whole genome
788 comparisons dramatically improves orthogroup inference accuracy. *Genome biology*.
789 2015;16(1):157.
- 790 101. Kolde R, Kolde MR. Package ‘pheatmap’. *R Package*. 2015;1(7).
- 791 102. Greening C, Biswas A, Carere CR, Jackson CJ, Taylor MC, Stott MB, et al. Genomic
792 and metagenomic surveys of hydrogenase distribution indicate H₂ is a widely utilised energy
793 source for microbial growth and survival. *The ISME journal*. 2016;10(3):761.
- 794 103. Katoh K, Standley DM. MAFFT multiple sequence alignment software version 7:
795 improvements in performance and usability. *Molecular Biology and Evolution*.
796 2013;30(4):772-80.
- 797 104. Stamatakis A. RAxML version 8: a tool for phylogenetic analysis and post-analysis of
798 large phylogenies. *Bioinformatics*. 2014;30(9):1312-3.

799 105. Letunic I, Bork P. Interactive tree of life (iTOL) v3: an online tool for the display and
800 annotation of phylogenetic and other trees. *Nucleic Acids Research*. 2016;44(W1):W242-W5.

801

802 **Tables and Figures**803 **Table 1. Characteristics of the metagenome-assembled genomes.**
804

Bin Id	Genome size (Mbp)	No. scaffolds	N50 (scaffolds; bp)	Strain heterogeneity [#]	Compl. (%) [#]	Cont. (%) [#]	GC	#CDS	Environment	Accession no.*	16S rRNA gene?
ASW-1	1.52	271	7,386	0.0	87.5	0.0	47.8	1946	Arsenic contaminated groundwater (Bangladesh)	SRR1563167, SRR1564103, SRR1573565, SRR1573578, SAMN10961276	N
ASW-2	2.63	157	28,058	25.0	94.4	4.8	48.0	2944	Arsenic contaminated groundwater (Bangladesh)	SRR1563167, SRR1564103, SRR1573565, SRR1573578, SAMN10961277	N
ASW-3	2.51	100	44,967	0.0	100.0	1.3	50.7	2892	Arsenic contaminated groundwater (Bangladesh)	SRR1563167, SRR1564103, SRR1573565, SRR1573578, SAMN10961278	N
ASW-4	2.24	155	24,336	0.0	97.1	0.7	43.2	2464	Arsenic contaminated groundwater (Bangladesh)	SRR1563167, SRR1564103, SRR1573565, SRR1573578, SAMN10961279	N
ASW-5	2.97	221	19,046	0.0	95.0	2.6	48.9	3353	Arsenic contaminated groundwater (Bangladesh)	SRR1563167, SRR1564103, SRR1573565, SRR1573578, SAMN10961280	N
ASW-6	2.19	68	56,691	66.7	99.4	2.0	46.6	2472	Arsenic contaminated groundwater (Bangladesh)	SRR1563167, SRR1564103, SRR1573565, SRR1573578, SAMN10961281	Y

BLZ1**	3.74	514	17,508	13.33	96.73	6.56	40.2	4659	AOM-nitrate reactor (Netherlands)	LKCM00000000.1	Y
BLZ2	3.74	85	74,304	0.0	99.4	4.6	40.3	4041	AOM-nitrate reactor (Netherlands)	GCA_002487355.1	N
CMD-1	1.85	116	27,949	100.0	98.0	0.7	44.9	2261	Copper mine tailings dam (Brazil)	SRR5161805, SRR5161795, SAMN10961282	N
CMD-2	1.45	221	9,704	0.0	88.4	0.0	44.1	1786	Copper mine tailings dam (Brazil)	SRR5161805, SRR5161795, SAMN10961283	N
HGW-1	2.00	128	24,496	33.3	96.4	2.0	43.2	2288	Groundwater samples (Japan)	GCA_002839545.1	Y
IPS-1	3.52	250	27,331	10.0	97.7	5.9	44.1	3970	Paddy field soil (Italy)	GCA_900196725.1	Y
M.Ferri	2.91	59	88,069	0.0	98.7	1.3	40.8	3019	AOM-iron reactor (Australia)	GCA_003104905.1	Y
M.Nitro	3.20	10	54,4976	0.0	99.7	1.3	43.2	3428	AOM-nitrate reactor (Australia)	GCA_000685155.1	Y
MGW-1	2.08	161	17,186	0.0	97.4	3.6	44.8	2488	Groundwater samples (Japan)	Not available [§]	N
Mn-1	3.59	68	87,551	0.0	100.0	1.3	40.6	3737	AOM-manganese reactor* (Australia)	SAMN10872768	N
Mn-2	3.32	116	49,809	0.0	99.4	4.6	42.9	3684	AOM-manganese reactor* (Australia)	SAMN10872769	N

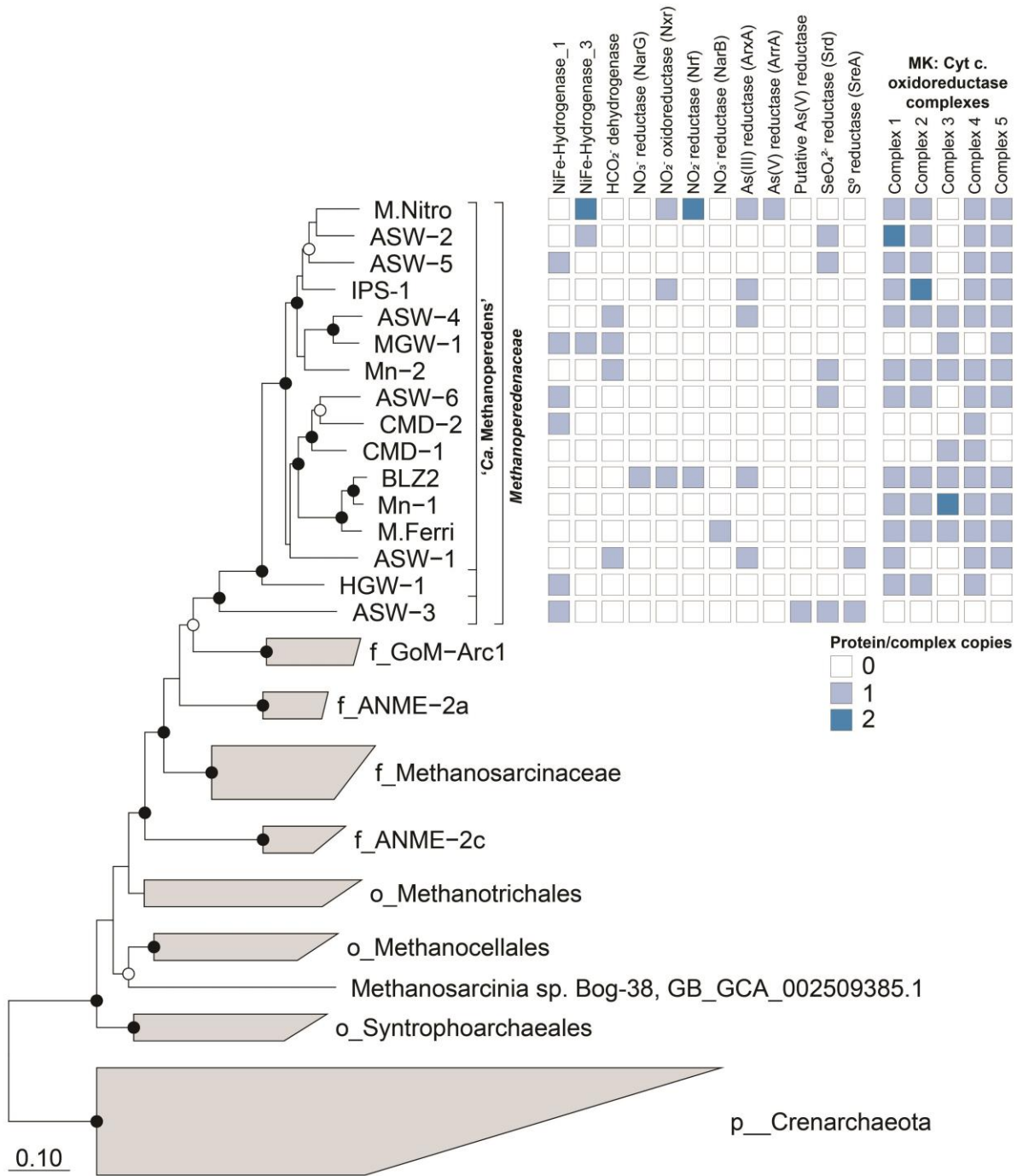
805 [#]Completeness (compl.), contamination (cont.), and strain heterogeneity were estimated using CheckM (33)

806 *Genome accession numbers. For the MAGs assembled in this study the SRA accession numbers are also given.

807 **The BLZ1 genome was not used in analyses as it is almost identical to the BLZ2 genome (99.5% ANI) and has inferior completeness and contamination values. The BLZ1
808 bioreactor was the parent system of the BLZ2 bioreactor.

809 [§]This genome was provided by Dr Yohey Suzuki and is associated with the study of HERNSDORF and colleagues (29)

810



811

812 **Figure 1. Phylogenetic placement of the *Methanoperedenaceae* MAGs and distribution**

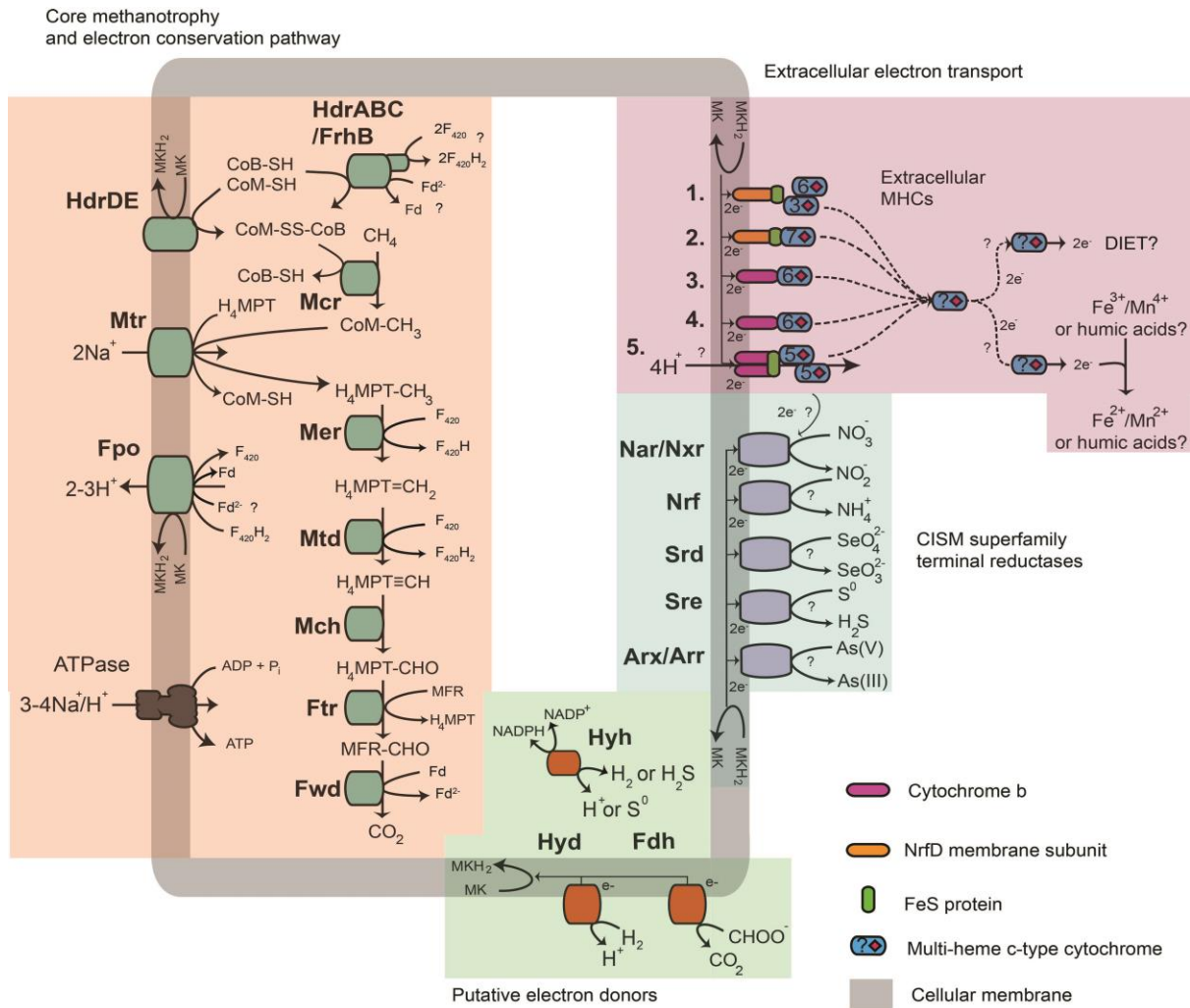
813 **of potential terminal electron acceptors.** The genome tree was inferred using maximum-

814 likelihood with a concatenated set of 122 archaeal specific marker genes. Black and white

815 dots indicate >90% and >70% bootstrap values, respectively. The scale bar represents amino

816 acids nucleotide changes. Based on GTDB-Tk the family *Methanoperedenaceae* includes

817 three genera including “*Ca. Methanoperedens*” which are denoted with brackets. The table to
818 the right of the tree shows the presence/absence of gene associated with potential terminal
819 electron acceptors in each corresponding *Methanoperedenaceae* genome.
820

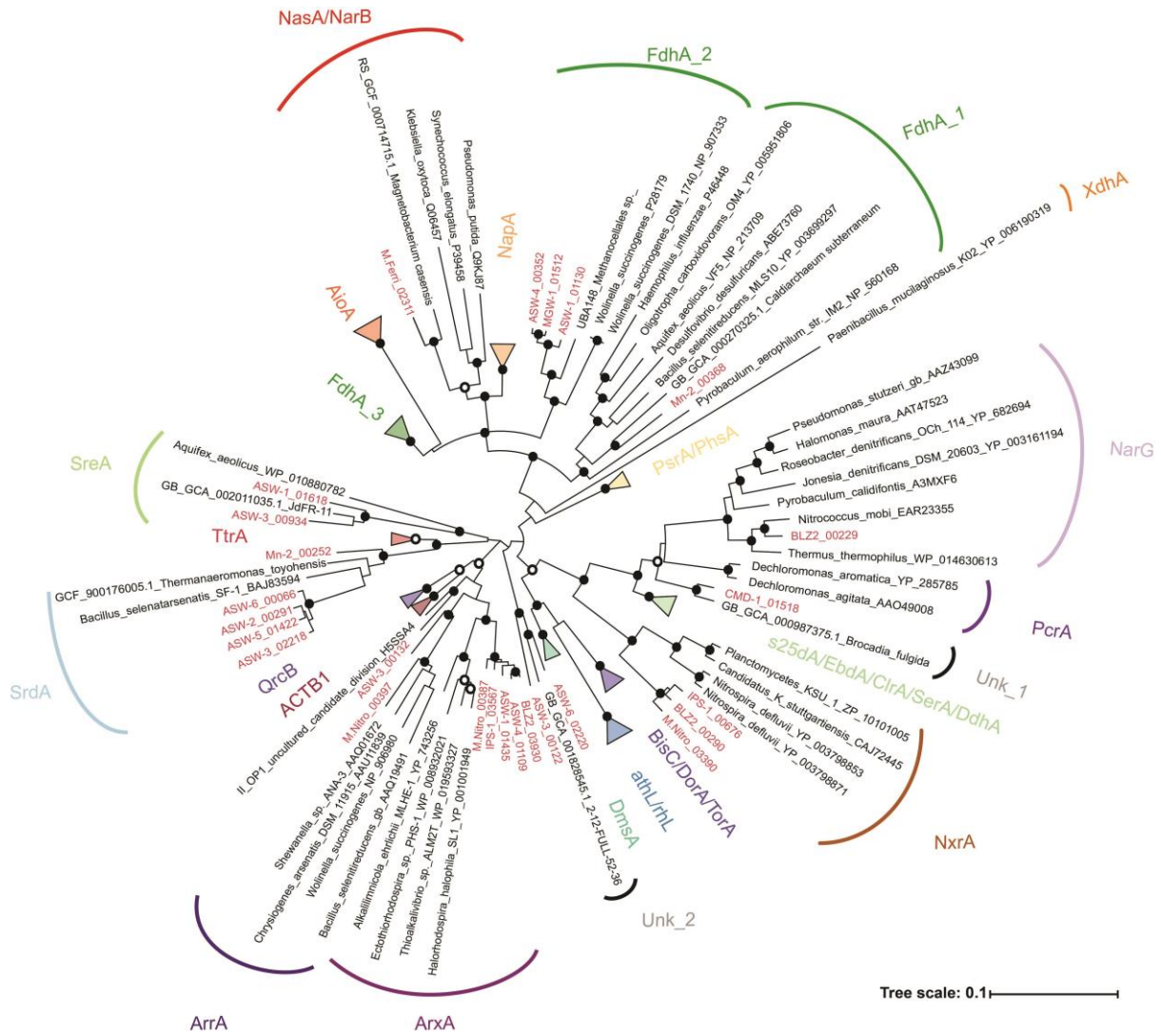


821

822 **Figure 2. Metabolic capabilities of the *Methanoperedenaceae*.** Key metabolic pathways for
 823 anaerobic oxidation of methane, energy conservation mechanisms, hydrogen and formate
 824 oxidation, and electron acceptors found within the pangenome of the *Methanoperedenaceae*.
 825 Numbers 1-5 indicate the different menaquinone:cytochrome c oxidoreductases conserved in
 826 the *Methanoperedenaceae* MAGs (**Dataset S1A**). Abbreviations for enzymes and co-factors
 827 in the figure are: H₄MPT, tetrahydromethanopterin; MFR, methanofuran; Fwd, formyl-
 828 methanofuran dehydrogenase; Ftr, Formylmethanofuran/H₄MPT formyltransferase; Mch,
 829 methenyl-H₄MPT cyclohydrolase; Mtd, F₄₂₀-dependent methylene H₄MPT dehydrogenase;
 830 Mer, F₄₂₀-dependent methylene-H₄MPT reductase; Mtr, Na⁺-translocating methyl-
 831 H₄MPT:coenzyme M methyltransferase; Mcr, methyl-coenzyme M reductase; F₄₂₀, F₄₂₀
 832 coenzyme; Fd, ferredoxin; CoM-SH, coenzyme M; CoB-SH, coenzyme B; Hdr,

833 heterodisulfide reductase; Fpo, F₄₂₀H₂ dehydrogenase; Hyd, type-1 NiFe hydrogenase; Hyh,
834 type-3b NiFe hydrogenase; Fdh, formate dehydrogenase; Nar, nitrate reductase; Nrf, nitrite
835 reductase, Ttr, tetrathionate reductase; Arx, arsenite oxidase; Arr, arsenate reductase;
836 DIET,direct interspecies electron transfer.

837



838

839 **Figure 3. Phylogenetic analysis of the catalytic subunits of the CISM superfamily.**

840 Putative genes recovered from the *Methanoperedenaceae* are highlighted in red. The gene

841 tree was inferred by maximum-likelihood and support values calculated via non-parametric

842 bootstrapping. Black and white dots indicate >90% and >70% bootstrap support, respectively.

843 The scale bar represents amino acid changes. ACTB1, alternate complex III, domain of

844 subunit B; ArrA, arsenate reductase; ArxA, arsenite oxidase; AthL, Pyrogallol

845 hydroxytransferase; BisC, biotin sulfoxide reductase; ClrA, chlorate reductase; EbdA,

846 Ethylbenzene dehydrogenase; s25dA, C25dehydrogenase; DmsA, DMSO reductase; DorA,

847 DMSO reductase; NapA, nitrate reductase; NarG, nitrate reductase; NasA, assimilatory

848 nitrate reductase; NarB, assimilatory nitrate reductase; NxrA, nitrite oxidoreductase; PsrA,

849 polysulfide reductase; PhsA, thiosulfate reductase; QrcB, quinone reductase complex; TtrA
850 tetrathionate reductase; DmsA, PcrA, perchlorate reductase; SrdA, Selenate reductase; SreA,
851 sulfreductase; TorA, TMAO reductase; XdhA, xanthine dehydrogenase; FdhA, formate
852 dehydrogenase; rhL, Resorcinol hydroxylase; Unk, unknown putative reductase. Amino acid
853 sequences are included in **Dataset S1B**.

854

855 **Supplemental material legends**

856 **Figure S1. Average amino acid identity (AAI%) for the *Methanoperedenaceae* genomes.**

857 AAI was calculated between each pair of genomes using CompareM.

858 **Figure S2. 16S rRNA gene based phylogenetic placement of the *Methanoperedenaceae***

859 **MAGs.** The 16S rRNA genes extracted from the *Methanoperedenaceae* MAGs from this
860 study are highlighted in red. Support values calculated via non-parametric bootstrapping. The
861 scale bar represents changes per nucleotide position.

862 **Figure S3. Phylogenetic analysis of methyl-coenzyme reductase subunit A (McrA).**

863 Putative genes recovered from the *Methanoperedenaceae* are highlighted in red. The gene
864 tree was inferred using maximum likelihood and support values calculated via non-
865 parametric bootstrapping. The scale bar represents amino acid changes.

866 **Figure S4. Phylogenetic analysis of the subunits of the NiFe hydrogenases annotated in**
867 **the *Methanoperedenaceae* genomes. A.** Analysis of the catalytic subunits of the energy-

868 converting NiFe hydrogenases. **B.** Analysis of the *b*-type cytochrome in the Group 1 NiFe
869 hydrogenases. Putative genes recovered from the *Methanoperedenaceae* are highlighted in
870 red. The gene trees were inferred using maximum likelihood and support values calculated
871 via non-parametric bootstrapping. The reference sequences of Group 1 and Group 3 NiFe
872 hydrogenases were acquired from Greening *et al.*, (C. Greening, A. Biswas, C. R. Carere, C.
873 J. Jackson, M. C. Taylor, M. B. Stott, G. M. Cook and S. E. Morales, ISME J 10: 761-777,
874 2016, <https://doi.org/10.1038/ismej.2015.153>) and the GTDB v83 reference sequences (D.H.
875 Parks, M. Chuvochina, D. W. Waite, C. Rinke, A. Skarshewski, P.-A. Chaumeil and P.
876 Hugenholtz, Nat Biotechnol 36: 996-1004, 2018, <https://doi.org/10.1038/nbt.4229>). The scale
877 bars represent amino acid changes.

878 **Figure S5. Subunit compositions of the Fpo dehydrogenase protein complexes and**
879 **theoretical bioenergetics of energy metabolism in ANME-2a and *Methanoperedenaceae*.**

880 **A.** Fpo subunit components for the ANME-2a and ASW-3 genomes (top left) and the other
881 members of the *Methanoperedenaceae* (bottom left). The utilization of different electron
882 carriers shows greater biochemical energetic gains based on more potential proton
883 translocation. The colours orange and green depict Methanosarcinales-like and non-
884 Methanosarcinales-like subunits. **B.** Theoretical redox potential drop when utilizing MP (left)
885 or MK (right) during F₄20H₂ and Fd²⁻ oxidation. This is due to differences between the
886 membrane-bound electron carriers' redox midpoint potential (E_m) of -80mV and -165mV for
887 MK and MP, respectively (M., Tietze, A. Beuchle, I. Lamla, N. Orth, M. Dehler, G. Greiner
888 and U. Beifuss, *Chembiochem* 4: 333-335, 2003, <https://doi.org/10.1002/cbic.200390053>;
889 Q.H. Tran and G. Uden, *Eur. J. of Biochem.* 251: 538-543, 1998,
890 <https://doi.org/10.1046/j.1432-1327.1998.2510538.x>).

891 **Figure S6. Phylogenetic analysis of the Fpo subunits annotated in the**

892 ***Methanoperedenaceae* genomes. A. FpoA B. FpoB C. FpoC D. FpoD E. FpoH F. FpoI G.**
893 **FpoJ1 H. FpoJ2 I. FpoK J. FpoL K. FpoM L. FpoN M. FpoO.** Putative genes recovered from
894 the *Methanoperedenaceae* are highlighted in red. The gene trees were inferred using
895 maximum likelihood and support values calculated via non-parametric bootstrapping.
896 Reference genes and the taxonomy are from the GTDB v83 database (D.H. Parks, M.
897 Chuvochina, D. W. Waite, C. Rinke, A. Skarszewski, P.-A. Chaumeil and P. Hugenholtz, *Nat*
898 *Biotechnol* 36: 996-1004, 2018, <https://doi.org/10.1038/nbt.4229>).

899 **Figure S7. Phylogenetic analysis of the subunits of the MK:cytochrome oxidoreductases**
900 **annotated in the *Methanoperedenaceae* MAGs. A. Analysis of the NrfD subunits. B.**

901 **Analysis of the b-type cytochromes.** Bootstrap values for the maximum-likelihood trees were

902 determined using non-parametric bootstrapping with 100 replicates. The scale bars represent
903 amino acid changes.

904 **Figure S8. Abundance profiles for the MHC orthologous protein families annotated in**
905 **the *Methanoperedenaceae* MAGs.**

906 **Figure S9. Network analysis of MHC orthologous protein families in**
907 ***Methanoperedenaceae*.** Each cluster represents related MHCs. The colour of the nodes
908 represents the taxonomic lineage based on GTDB classification. The size of the nodes
909 represents the number of CXXCH heme binding motifs identified in the proteins. The
910 thickness of the lines represents amino acid identity between the two nodes. The shaded
911 boxes represent the orthologous protein families.

912 **Dataset S1. Sequences, identifiers and statistics for genes used in the comparative**
913 **analyses of the *Methanoperedenaceae* MAGs. A.** Genes encoding proteins involved in the
914 methane oxidation pathway, energy conservation, and other metabolic pathways as shown in
915 Figure 2. **B.** Amino acid sequences used in the CISM superfamily gene tree (Figure 3).
916 Amino acid sequences include curated sequences from Swiss-Prot and Castelle *et al.*, (C.J.
917 Castelle, L. A. Hug, K. C. Wrighton, B. C. Thomas, K. H. Williams, D. Wu, S. G. Tringe, S.
918 W. Singer, J. A. Eisen and J. F. Banfield, Nat commun 4: 2120, 2013,
919 <https://doi.org/10.1038/ncomms3120>) and closely related sequences from GTDB r83 protein
920 reference database (D.H. Parks, M. Chuvochina, D. W. Waite, C. Rinke, A. Skarszewski, P.-
921 A. Chaumeil and P. Hugenholtz, Nat Biotechnol 36: 996-1004, 2018,
922 <https://doi.org/10.1038/nbt.4229>). **C.** Amino acid sequences used in the catalytic subunits of
923 the energy-converting NiFe hydrogenase. Amino acid sequences include curated sequences
924 from Greening *et al.*, (C. Greening, A. Biswas, C. R. Carere, C. J. Jackson, M. C. Taylor, M.
925 B. Stott, G. M. Cook and S. E. Morales, ISME J 10: 761-777, 2016,

926 <https://doi.org/10.1038/ismej.2015.153>) and closely related sequences from GTDB r83
927 protein reference database. **D.** Genes encoding putative NiFe hydrogenase maturation
928 proteins. **E.** Best blastp hits of Fpo dehydrogenase subunits to the IMG database. Blastp hits
929 shows divergent Fpo subunits are present in the *Methanoperedeneceae* MAGs as seen in
930 Figure S6. Top blast hits to Methanoperedens-like protein sequences were excluded. **F.**
931 General statistic of multi-heme *c*-type cytochromes (MHCs) in the ANME genomes. **G.**
932 MHC general statistics for all bacterial and archaeal families in the GTDB v89 database.
933